

# 複晶矽薄膜電晶體之晶粒結構與光漏電之分析

研究生：魏全生

指導教授：冉曉雯 教授

國立交通大學

顯示科技研究所碩士班

## 中文摘要

本論文主要探討複晶矽薄膜電晶體光漏電的現象。當複晶矽薄膜電晶體應用在主動式液晶顯示器時,會受到背光的影響產生光漏電,導致畫素電壓的下降和串音的增加。目前的研究上指出,複晶矽薄膜電晶體的光漏電主要在汲極空乏區產生,由於光子能量被矽膜吸收後,激發價帶電子躍遷到傳導帶形成電子電洞對,此電子電洞對在空乏區內建電場影響下,會分開向相反方向移動形成光電流。為了探討這樣的光吸收效應和矽薄膜品質有無關係,我們在實驗中特別利用雷射再結晶技術,改變雷射能量產生不同晶粒的複晶矽薄膜,這使我們可以進一步分析光電流在不同晶粒大小上的影響。同時,我們也調整複晶矽薄膜電晶體的通道長度、通道寬度以及輕汲極摻雜(LDD)長度來探討元件尺寸及空乏區變化對光漏電的影響,針對LDD長度對暗態漏電以及光漏電的不同影響,我們也提出討論以及定義出最佳的LDD長度。

另外,由於色序法技術的發展,背光將以紅綠藍色光依序發光,但對於不同色光產生的光漏電尚無人探討,我們預期這對複晶矽薄膜電晶體的光漏電會造成不同的影響,因此本論文也針對不同紅綠藍色光在複晶矽薄膜電晶體上造成的光漏電作研究。我們利用簡單的濾光膜產生紅藍綠不同色光的光源,調整光源強

度，然後計算其不同色光下的光子數目，可以更深入的探討光電流效應。



# **Grain Size Effect and the Photo Leakage Current of Poly-Si TFTs**

Student : Chung-Sheng Wei

Advisor : Dr. Hsiao-Wen Zan

Institute of Display  
National Chiao Tung University

## **Abstract**

In this paper, the photo leakage current of poly-Si thin film transistors (poly-Si TFTs) are studied. Since poly-Si TFTs are widely used in active-matrix liquid crystal displays (AMLCD), they usually will be exposed to the scattered light from the backlight system. The photon energy will be absorbed by the silicon film to excite the generation of electron-hole pairs. Under certain electric field such as the built-in electric field in the depletion regions, the electron and the hole will move toward the opposite direction and form the current. Compared to the generation current from the depletion region in the dark environment, this light-caused current is much larger and causes pronounced leakage current issues.

In our experiment, we try to study the influence of poly-Si film properties on the photo leakage current. We change the laser energy in the laser recrystallization process to obtain poly-Si films with various grain sizes. These films are used to serve as the active layer in the poly-Si TFTs. The influence of grain size on the photo leakage current is therefore can be measured. Also, various channel length, channel width and the lightly-doped drain (LDD) length are also designed. Their influences on the photo leakage current are also investigated.

Since the color sequential technology has been proved to be an effective method to

greatly improve the luminance of the displays, backlight system generates blue, red, and green light at different time is an unavoidable trend. However, the photo leakage current of poly-Si TFTs under different Red 、 Green 、 Blue light sources has not been studied before. In our experiment, we also try to produce the RGB light sources by using simple filtering films on the CCFL backlight system. The measured photo leakage current under different light sources are compared. The simulated results consider both the photon number per second and also the absorption coefficient are compared with the experimental results.



## Acknowledgement 誌謝

口試結束後的驚喜與悸動，我想是我人生中不能忘懷的回憶，二年來的學習過程中，有歡笑也有挫折，在這過程當中，有許多人我要謝謝他們一路上的陪伴。首先我要感謝我的家人與指導教授 冉曉雯老師，在我學習過程及平日生活當中，所給予的關懷與鼓勵，讓我能夠逐一的解除迷惑。

接著，要感謝 國錫學長、士欽學長、銘龍學長、陳均衡學長平時的照顧，以及在我研究上有問題時，所給予的解答與幫助讓我受益良多，以及一起奮鬥的伙伴，章祐、貞儀、庭軒、溥寬、傑斌，有你們的幫助使的兩年內的學習生活當中，獲益良多，最後，謝謝學弟平日的配合與帶來實驗室無比的歡樂，讓這兩年的碩士生活當中，更加的多采多姿。

魏全生 於交大電資 805

2006 06 26

# Contents

<b>Chinese Abstract</b>	<b>I</b>
<b>English Abstract</b>	<b>III</b>
<b>Acknowledgment</b>	<b>V</b>
<b>Contents</b>	<b>VI</b>
<b>Figure Capions</b>	<b>X</b>
<b>Table Capions</b>	<b>XII</b>
<b>Appendix</b>	<b>XIII</b>

## **Chapter 1. Introduction**

1-1 An Overview of LTPS Technology	1
1-2 Photo leakage current of Poly-Si films	3
1-3 Motivation	4
1-4 Thesis Outline	4

## **Chapter 2. Analysis of Activation Energy for Poly-Si TFTs**

2-1 Device fabrication and measurement	6
2-2 Parameter extraction	7
2-3 Material analysis	9
2-4 Device characterization	10
2-5 Grain barrier height model	11
2-6 Activation Energy Analysis	13
2-7 Trap State Density Analysis	14

## **Chapter 3. Characteristics of Photo Leakage Current for Poly-Si TFTs**

3-1 Optical absorption	15
3-2 Photo leakage current	16

3-3 Photo Current of Poly-Si TFTs with Illumination of RGB color	18
3-4 Optical properties of poly-Si film	19
3-5 Simulation of photon number per second with the illumination of Red, Green,Blue color into the poly-Si film	20
<b>Chapter 4. Conclusion</b>	<b>22</b>
<b>Reference</b>	<b>24</b>



# Figure Captions

## Chapter 2.

Fig. 2-1 Schematic cross-sectional view of poly-Si TFT.

Fig. 2-3 SEM image of different laser energy density in the channel thickness of 100nm.

Fig2-4-1(a) Process window of field effect mobility with different channel thickness utilizing solid state laser crystallization. (  $W/L = 6\mu m / 30\mu m$  )

Fig2-4-1(b) Process window of threshold voltage with different channel thickness utilizing solid state laser crystallization. (  $W/L = 6\mu m / 30\mu m$  )

Fig2-4-1(c) Process windows of subthreshold swing with different channel thickness utilizing solid state laser crystallization . (  $W/L = 6\mu m / 30\mu m$  )

Fig.2-4-3(a) Transfer characteristics of different grain size and film quality for  $V_{DS}=2.1V$ . (  $W/L = 6\mu m / 30\mu m$  )

Fig.2-4-3(b) Transfer characteristics of different grain size and film quality for  $V_{DS}=6.1V$ . (  $W/L = 6\mu m / 30\mu m$  )

Fig.2-5-1 Arrhenius plot of the drain current of  $W/L = 6\mu m / 30\mu m$  n-channel device for different drain voltages. The slope of each line defines the activation energy (  $E_a$  ).

Fig.2-5-2 The experimental inverse of grain barrier height versus the gate voltage for different grain growth conditions. (  $W/L = 6\mu m / 30\mu m$  )

Fig 2-5-3 The relationship of Activation energy with different grain size and film quality. (  $W/L = 6\mu m / 30\mu m$  )

Fig. 2-5-4 The relationship of activation energy with different grain size and film quality at the channel for  $V_{DS}=0.1V$ . (  $W/L = 6\mu m / 30\mu m$  )

Fig. 2-5-5 Plot of  $\ln [ I_{DS} / ( V_G - V_{FB} ) V_{DS} ]$  against both  $1 / ( V_G - V_{FB} )^2$ , used to



determine  $Nt$  at the different grain size and the film quality. (  $W/L = 6\mu m / 30 \mu m$  )

Fig.2-5-6 Trap State Density utilizing the solid state laser to crystallization with the different grain size and different dimension.

### Chapter 3.

Fig. 3-1 Incident photon intensity distribution as the thickness variation.

Fig. 3-2 Characteristics of drain current with various illumination of poly-Si TFTs. SSL device with the channel thickness  $50nm$  and grain size  $1\mu m$  at the  $V_{DS}=2.1V$ .

Fig. 3-3 Characteristics of drain current with illumination of  $6000 ( cd/m^2 )$ . SSL device with the channel thickness  $100nm$  and grain size  $0.3\mu m$  at the  $V_{DS}=2.1V$  and  $V_{GS}= -3 V$ .

Fig. 3-4 Characteristics of drain current with the illumination of  $6000 (cd/m^2)$ . SSL device with the channel thickness  $100nm$  and grain size  $0.3\mu m$  at the  $V_{DS}=2.1V$  and  $V_{GS}= -3 V$ .

Fig. 3-5 Dependence of photo leakage current with different channel width at the channel length  $6 \mu m$ . SSL device with the channel thickness  $50nm$  at the  $V_{DS}=2.1V$  and  $V_{GS}= -3 V$ .

Fig. 3-6 Dependence of photo leakage current with different channel length at the channel width  $6 \mu m$ . SSL device with the channel thickness  $50nm$  at the  $V_{DS}=2.1V$  and  $V_{GS}= -3 V$ .

Fig.3-7 Dependence of the photo leakage current on various LDD lengths. SSL device with the channel thickness  $50nm$  at the  $V_{DS}=4.1V$  and  $V_{GS}= -4 V$  (  $W/L=30 \mu m/30 \mu m$  ).

Fig.3-8 Dependence of photo leakage current on the different grain size with the

illumination of  $6000 \text{ (cd/m}^2\text{)}$ . SSL device with the channel thickness  $50\text{nm}$  at the  $V_{DS}=2.1\text{V}$  and  $V_{GS}= -3 \text{ V ( } W/L=30 \mu\text{m}/30 \mu\text{m )}$ .

Fig.3-9 Dependence of the photo leakage current on the different channel thickness with the illumination of  $6000 \text{ ( cd/m}^2\text{)}$ . SSL device with the grain size  $0.6\mu\text{m}$  at the  $V_{DS}=2.1\text{V ( } W/L=30 \mu\text{m}/30 \mu\text{m )}$ .

Fig.3-10 Color coordinate of RGB-LED.

Fig.3-11 Wavelength characteristics of white light LED.

Fig.3-12 Wavelength characteristic of CCFL backlight.

Fig.3-13 Wavelength characteristic of CCFL backlight with the RGB filter.

Fig.3-14 The color coordinate of RGB color.

Fig.3-15 Dependence of various grain size of photo leakage current with the illumination of RGB color. SSL device with the channel thickness  $50\text{nm}$  at the  $V_{DS}=2.1\text{V}$  and  $V_{GS}= -3 \text{ V ( } W/L = 30 \mu\text{m}/30 \mu\text{m )}$ .

Fig.3-16 Extinction coefficient of different channel thickness.

Fig.3-17 Refractive index of different channel thickness.

Fig.3-18 Absorbance coefficient of poly-Si film.

Fig.3-19 Absorptivity of the SSL films with different grain size at the channel thickness  $50\text{nm}$ .

Fig.3-20 Absorptivity of the SSL films with different channel thickness.

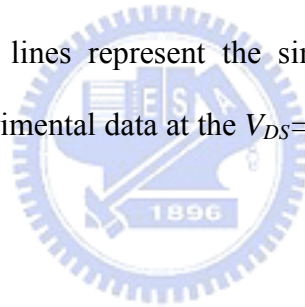
Fig.3-21 Absorptivity of different channel thickness from ref [20]. Where 111 、 112 、 113 、 114 、 115 represent the channel thickness of  $30\text{nm}$  、  $50 \text{ nm}$  、  $70 \text{ nm}$  、  $90 \text{ nm}$  and  $110 \text{ nm}$  respectively.

Fig.3-22 Simulation of photon number per second with the illumination of different radiant flux. Compare with the photo leakage with the illumination of RGB color on the SSL device with the channel thickness  $50\text{nm}$  and grain size= $1\mu\text{m}$ . The lines represent the simulated result and the symbol

represent the experimental data at the  $V_{DS}=2.1V$  and  $V_{GS}= -3 V$  (  $W/L = 30 \mu m/30 \mu m$  ).

Fig.3-23 Simulation of photon number per second with the illumination of different radiant flux. Compare with the photo leakage with the illumination of RGB color on the SSL device with the channel thickness  $50nm$  and grain size= $0.55\mu m$ . The lines represent the simulated result and the symbol represent the experimental data at the  $V_{DS}=2.1V$  and  $V_{GS}= -3 V$  (  $W/L = 30 \mu m/30 \mu m$  ).

Fig.3-24 Simulation of photon number per second with the illumination of different radiant flux. Compare with the photo leakage with the illumination of RGB color on the ELA device with the channel thickness  $50nm$  and grain size= $0.3 \mu m$ . The lines represent the simulated result and the symbol represent the experimental data at the  $V_{DS}=2.1V$  and  $V_{GS}= -3 V$  (  $W/L = 30 \mu m/30 \mu m$  ).



## Table Captions

**Table I** Devices turn on parameter of different grain size and film quality.

**Table II**  $\gamma$  Value for different grain growth conditions.

**Table III** Trap state density with different grain size.

**Table IV** Radiant Flux Intensity (*Watt*) of RGB-LED.



## Appendix XIII

Calculated of Radiant Flux intensity

$$x = \frac{X}{X + Y + Z}$$

$$y = \frac{Y}{X + Y + Z}$$

$$\therefore X = x(X + Y + Z) = x(Y / y)$$

$$Y = Y$$

$$Z = z(X + Y + Z) = (1 - x - y)(Y / y)$$

Where  $X$  ,  $Y$  ,  $Z$  represents the tristimulus and  $x$   $y$  is color coordinate.

$$R(Y_r, x_r, y_r) \cdot G(Y_g, x_g, y_g) \cdot B(Y_b, x_b, y_b)$$

$$X = x_r(Y_r / y_r) + x_g(Y_g / y_g) + x_b(Y_b / y_b)$$

$$Y = Y_r + Y_g + Y_b$$

$$X + Y + Z = Y_r / y_g + Y_g / y_g + Y_b / y_b$$

Where  $R(Y_r, x_r, y_r)$  represents the

Luminance of red:  $Y_r$

Color coordinate of red ( $x_r, y_r$ )

$G(Y_g, x_g, y_g)$  represents the

Luminance of green:  $Y_g$

Color coordinate of green ( $x_g, y_g$ )

Luminance of blue:  $Y_b$

Color coordinate of blue ( $x_b, y_b$ )



$$x = X / (X + Y + Z) = \frac{[x_r(Y_r / y_r) + x_g(Y_g / y_g) + x_b(Y_b / y_b)]}{(Y_r / y_r) + (Y_g / y_g) + (Y_b / y_b)} \quad (1-2)$$

$$y = Y / (X + Y + Z) = \frac{(Y_r + Y_g + Y_b)}{(Y_r / y_r) + (Y_g / y_g) + (Y_b / y_b)}$$

And the color coordinate of the color addition as show in equation (1-2), it is dependence on the luminance of RGB color and color coordinate of RGB color.

Because the photo luminance has to transform the luminance ( $lm/sr\text{-}cm^2$ ) in unit to the radiant flux ( $Watt/sr\text{-}cm^2$ ), so the transform of radiant flux can be obtained from

equation (1-3).

$$Y = L = Km \int R_{\lambda} V(\lambda) d\lambda$$

where  $Km = 683 \text{ lm/W}$  (1-3)

$Km' = 1700 \text{ lm/W}$

As seen in figure 1, green light at the wavelength of 555nm defines the value of km which is equal to 683 ( lm/W). So, the calculated of radiant flux was obtained in table

IV

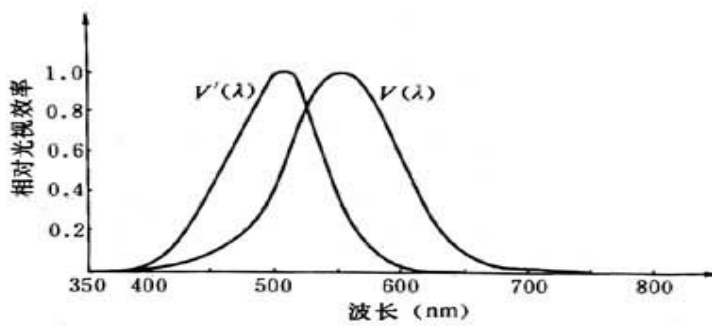


图1 CIE 相对光谱光视效率曲线  $V(\lambda)$ (明视觉)和  $V'(\lambda)$ (暗视觉)

